Article

Immunity

mTORC1 and mTORC2 Kinase Signaling and Glucose Metabolism Drive Follicular Helper T Cell Differentiation

Graphical Abstract

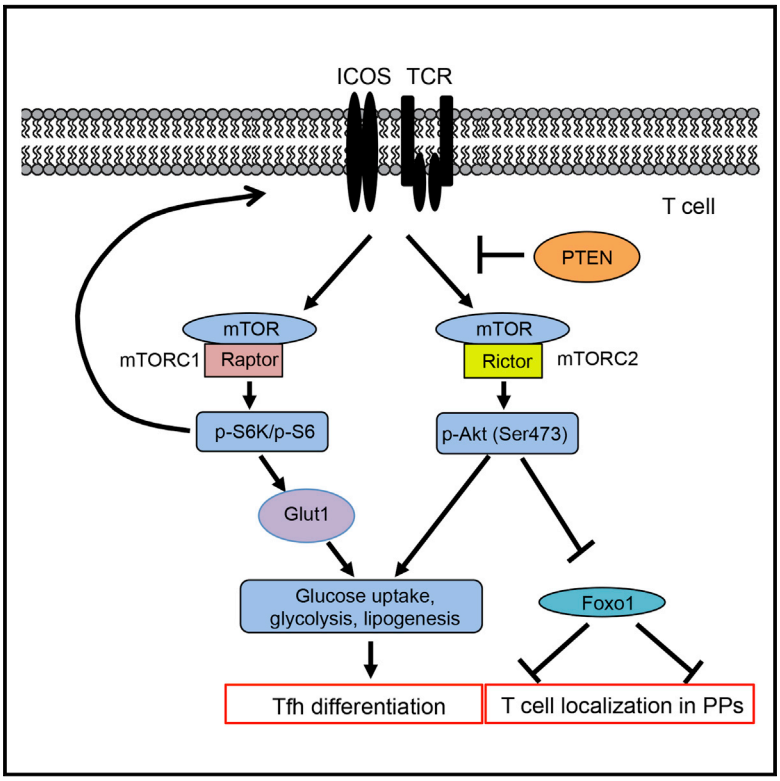

Authors

Hu Zeng, Sivan Cohen, Cliff Guy, ..., Jason W. Locasale, Jeffrey C. Rathmell, Hongbo Chi

Correspondence

jeff.rathmell@vanderbilt.edu (J.C.R.), hongbo.chi@stjude.org (H.C.)

In Brief

Follicular helper T (Tfh) cells are essential for efficient humoral immune responses. Zeng et al. identify mTOR signaling and glucose metabolism as critical regulators of Tfh cell differentiation in response to foreign antigen challenge and at steady state in Peyer's patches.

Highlights

- Raptor or Rictor deletion impairs GC and Tfh responses and IgA production
- mTORC2 but not mTORC1 signals via Foxo1 inhibition to drive Tfh cell differentiation
- mTORC1 and mTORC2 promote foreign antigen and LCMV-induced GC and Tfh responses
- mTOR links ICOS and Glut1 to anabolic metabolism for Tfh cell differentiation

Accession Numbers

GSE85555

Zeng et al., 2016, Immunity *45*, 540–554
September 20, 2016
http://dx.doi.org/10.1016/j.immuni.2016.08.017

CellPress

Immunity
Article

mTORC1 and mTORC2 Kinase Signaling and Glucose Metabolism Drive Follicular Helper T Cell Differentiation

Hu Zeng,[1,6] Sivan Cohen,[2,6] Cliff Guy,[1] Sharad Shrestha,[1] Geoffrey Neale,[3] Scott A. Brown,[1] Caryn Cloer,[1] Rigel J. Kishton,[2] Xia Gao,[2] Ben Youngblood,[1] Mytrang Do,[4] Ming O. Li,[4] Jason W. Locasale,[2] Jeffrey C. Rathmell,[2,5,7,*] and Hongbo Chi[1,7,8,*]

[1]Department of Immunology, St. Jude Children's Research Hospital, Memphis, TN 38105, USA
[2]Department of Pharmacology and Cancer Biology, Duke University, Durham, NC 27710, USA
[3]Hartwell Center for Bioinformatics and Biotechnology, St. Jude Children's Research Hospital, Memphis, TN 38105, USA
[4]Immunology Program, Memorial Sloan Kettering Cancer Center, New York, NY 10065, USA
[5]Department of Pathology, Microbiology, and Immunology, and Center for Immunobiology, Vanderbilt University Medical Center, Nashville, TN 37232, USA
[6]Co-first author
[7]Co-senior author
[8]Lead contact
*Correspondence: jeff.rathmell@vanderbilt.edu (J.C.R.), hongbo.chi@stjude.org (H.C.)
http://dx.doi.org/10.1016/j.immuni.2016.08.017

SUMMARY

Follicular helper T (Tfh) cells are crucial for germinal center (GC) formation and humoral adaptive immunity. Mechanisms underlying Tfh cell differentiation in peripheral and mucosal lymphoid organs are incompletely understood. We report here that mTOR kinase complexes 1 and 2 (mTORC1 and mTORC2) are essential for Tfh cell differentiation and GC reaction under steady state and after antigen immunization and viral infection. Loss of mTORC1 and mTORC2 in T cells exerted distinct effects on Tfh cell signature gene expression, whereas increased mTOR activity promoted Tfh responses. Deficiency of mTORC2 impaired CD4$^+$ T cell accumulation and immunoglobulin A production and aberrantly induced the transcription factor Foxo1. Mechanistically, the costimulatory molecule ICOS activated mTORC1 and mTORC2 to drive glycolysis and lipogenesis, and glucose transporter 1-mediated glucose metabolism promoted Tfh cell responses. Altogether, mTOR acts as a central node in Tfh cells by linking immune signals to anabolic metabolism and transcriptional activity.

INTRODUCTION

Follicular helper T (Tfh) cells are specialized effector T cells that stimulate B cells in germinal center (GC) follicles to produce long-lived high-affinity immunoglobulins (Crotty, 2014). Tfh cells are defined by expression of the transcription factor Bcl6, chemokine receptor CXCR5, and surface receptors PD-1 and ICOS. Differentiation of Tfh cells requires T cell interaction with dendritic cells and B cells and signaling by ICOS and cytokines (Crotty, 2014). Although the GC response is usually induced by foreign antigen stimulation in peripheral lymphoid organs, it is continuously present in Peyer's patches (PPs) and contributes to the production of secretive immunoglobulin A (IgA) for gut immune homeostasis. This spontaneous GC formation is maintained by perpetual exposure to gut microbiota and strictly depends upon Tfh cell help (Fagarasan et al., 2010). GC formation and Tfh cell development in PPs are abrogated in ICOS-deficient mice (Gigoux et al., 2009; Iiyama et al., 2003), illustrating the essential role of ICOS in both peripheral and mucosal Tfh cell differentiation. However, signaling mechanisms underlying Tfh cell differentiation, particularly in PPs, remain essentially unexplored.

T cell differentiation is accompanied by dynamic metabolic reprogramming (MacIver et al., 2013). One of the crucial regulators of anabolic metabolism is mechanistic target of rapamycin (mTOR) signaling, which is composed of two distinct kinase complexes, mTOR complex 1 (mTORC1) and 2 (mTORC2) that are characterized by the signature components Raptor and Rictor, respectively (Chi, 2012). Recent studies have revealed discrete functions of mTORC1 and mTORC2 in effector CD4$^+$ T cell differentiation (Chi, 2012). The metabolic function of mTOR signaling in T cells has been mainly ascribed to mTORC1 (Finlay et al., 2012; Yang et al., 2013; Zeng et al., 2013), while mTORC2 negatively controls anabolic metabolism in CD8$^+$ T cells (Pollizzi et al., 2015). A recent study shows that shRNA-mediated silencing of mTOR or Raptor, but not Rictor, in activated T cells enhances Tfh cell differentiation (Ray et al., 2015), indicating an inhibitory role of mTORC1 and metabolism in Tfh cell differentiation. However, this conclusion appears to be contrary to the positive roles of PI3K signaling in Tfh cell responses (Gigoux et al., 2009; Rolf et al., 2010). Furthermore, Bcl6 has been shown to directly inhibit glycolytic genes in T helper 1 (Th1) and CD8$^+$ T cells (Oestreich et al., 2014). Yet, Bcl6^{hi} Tfh cells show higher proliferation and increased expression of cell-cycle-related genes compared to Bcl6^{lo} Tfh cells (Kitano et al., 2011), and Tfh cells also exhibit a higher rate of proliferation

than other effector T cells (Lüthje et al., 2012). Finally, expression of the glucose transporter Glut1 and increased glycolysis have been shown to promote effector T cell function and proliferation (Jacobs et al., 2008; Macintyre et al., 2014). Detailed metabolic requirements and the interplay with signaling events in Tfh cells, however, remain to be established.

Here we tested the role of mTORC1 and mTORC2 and glucose metabolism in Tfh cell differentiation and the ability to promote GC responses. We found that both mTORC1 and mTORC2 were crucial positive determinants of Tfh and GC responses by orchestrating discrete transcriptional programs. mTORC1 and mTORC2 were activated by ICOS to promote metabolism including glycolysis and lipogenesis, while mTORC1 also directly contributed to ICOS expression. Importantly, direct manipulation of metabolic activities through the transcription factor Myc or Glut1 modulated Tfh cell responses. Our study demonstrates that mTORC1 and mTORC2 play non-redundant roles in Tfh cell differentiation by linking immune signals to anabolic metabolism and transcriptional activity.

RESULTS

mTOR Signaling Is Sufficient and Necessary for GC and Tfh Responses in PPs

To investigate how mTOR signaling shapes GC and Tfh cell responses under steady state, we examined PPs from *Cd4*^{cre}*Pten*$^{fl/fl}$ mice with T cell-specific deletion of PTEN, a crucial negative regulator of PI3K and mTOR signaling (Chi, 2012). PPs from wild-type (WT) mice contained a sizable population of B cells expressing GC markers GL-7 and Fas, and of T cells expressing Tfh cell markers PD-1 and CXCR5 (Figures 1A and 1B). PTEN deficiency significantly increased the frequencies of GC B cells and Tfh cells in PPs (Figures 1A and 1B). Because PTEN also possesses functions independent of PI3K-Akt (Shen et al., 2007; Song et al., 2011), we used *Cd4*-Cre to ectopically express a constitutively active form of the PI3K catalytic subunit p110α (encoded by *Pik3ca*) (Srinivasan et al., 2009) in T cells (referred to as *Pik3ca**). GC B cell and Tfh cell frequencies were markedly enhanced in *Cd4*^{cre}*Pik3ca** mice (Figures S1A and S1B). Next, to test the requirement of mTOR, we treated WT mice with rapamycin, an immunosuppressant that targets mTORC1 primarily but also mTORC2 under long-term treatment (Chi, 2012). Rapamycin strongly reduced GC B and Tfh cells in PPs (Figure 1C). Therefore, over-activation of PI3K-mTOR and inhibition of mTOR exert positive and negative effects on GC B and Tfh cells in PPs, respectively.

Although PI3K-Akt is a classical activator of mTOR (Chi, 2012), PI3K-Akt-independent pathways of mTOR activation have been identified (Deane et al., 2007; Donahue and Fruman, 2007; Finlay et al., 2012). To establish the roles of mTOR and to dissect the two mTOR complexes in this process, we generated *Cd4*^{cre}*Rptor*$^{fl/fl}$ and *Cd4*^{cre}*Rictor*$^{fl/fl}$ mice and examined T cell homeostasis and GC responses in PPs. Compared with splenic T cells, T cells from PPs contained a considerably higher frequency of CD44^{hi}CD62L^{lo} memory-phenotype (MP) T cells (Figure S1C). In PPs, Rictor deficiency resulted in a more pronounced reduction of MP T cells than Raptor deficiency (Figure S1D), suggesting a preferential role for mTORC2 in PPs. Indeed, we observed a reduced frequency and number of CD4^{+} T cells in PPs from *Cd4*^{cre}*Rictor*$^{fl/fl}$ mice, but not from *Cd4*^{cre}*Rptor*$^{fl/fl}$ mice (Figure 1D and Figure S1E). We next examined GC B cells and Tfh cells, and found that the frequencies of these populations were significantly reduced in *Cd4*^{cre}*Rptor*$^{fl/fl}$ or *Cd4*^{cre}*Rictor*$^{fl/fl}$ mice (Figures 1E and 1F). Therefore, both mTORC1 and mTORC2 are required for Tfh cell generation in PPs, with mTORC2 making an additional contribution to T cell accumulation in PPs.

A unique feature of B cell responses in GCs of PPs is the switching of B cell isotype from IgM to IgA to maintain intestinal homeostasis (Fagarasan et al., 2010). Staining of surface IgA showed significantly reduced IgA expression on B cells from *Cd4*^{cre}*Rictor*$^{fl/fl}$ mice (Figure 1G). Moreover, *Cd4*^{cre}*Rictor*$^{fl/fl}$ mice had reduced IgA concentration in fecal extracts (Figure 1H). B cell IgA expression and fecal IgA production were trended lower in *Cd4*^{cre}*Rptor*$^{fl/fl}$ than WT mice, but the changes were smaller or did not reach statistical significance (Figures 1G and 1H). Thus, mTORC2 plays a prominent role in IgA production in PPs.

T follicular regulatory T cells (Tfr) constrain Tfh cell differentiation (Chung et al., 2011; Linterman et al., 2011), and so the diminished Tfh cells in PPs in Raptor or Rictor-deficient mice could be due to elevated Tfr cell function. However, Raptor deficiency in Treg cells abrogates their suppressive function (Zeng et al., 2013) and is unlikely to account for the diminished Tfh cells in *Cd4*^{cre}*Rptor*$^{fl/fl}$ mice. To examine whether mTORC2 in Treg cells could affect Tfh cell differentiation, we analyzed *Cd4*^{cre}*Rictor*$^{fl/fl}$ mice and observed normal Tfr cells in PPs (Figure S1F). Also, Treg-specific deletion of Rictor via *Foxp3*-Cre had little effect on Tfh and GC B cells in PPs (Figure S1G). The blunted Tfh cell differentiation in Raptor or Rictor-deficient mice is thus unlikely to arise from Tfr cell functional enhancement.

mTOR in Activated T Cells Is Critical for Tfh Cell Differentiation and GC Formation in PPs

Because mTORC1 is required for early T cell activation (Yang et al., 2013), compromised T cell activation in the *Cd4*-Cre-mediated gene deletion could complicate data interpretation. We therefore used a deleter line with Cre expression mediated by the OX40 promoter to induce deletion in CD4^{+} T cells after initial activation (Kang et al., 2013). As expected, Raptor and Rictor mRNA were not completely depleted in CD4^{+} T cells until 3 days after in vitro activation (Figure 2A). Also, CD4^{+} T cells from OX40^{cre}*Rptor*$^{fl/fl}$ and OX40^{cre}*Rictor*$^{fl/fl}$ mice had largely normal proliferation within the first 2 days of stimulation (Figure 2B).

MP T cells are known to express OX40 (Klinger et al., 2009). In OX40^{cre} mice crossed with a Cre recombination reporter, efficient deletion of the reporter allele was observed in MP but not naive CD4 T cells in PPs (Figure S2A). PPs from OX40^{cre}*Rictor*$^{fl/fl}$ but not OX40^{cre}*Rptor*$^{fl/fl}$ mice contained a smaller population of CD4^{+} MP T cells than their WT counterparts (Figure S2B). Confocal microscopic examination of PPs from OX40^{cre}*Rptor*$^{fl/fl}$ and OX40^{cre}*Rictor*$^{fl/fl}$ mice revealed highly reduced staining with peanut agglutinin (PNA), a specific dye for GCs (Figure 2C). Flow cytometry analysis verified markedly reduced GC B and Tfh cells in PPs from these mice (Figures 2D and 2E). In contrast, T cell proliferation and apoptosis (data not shown) and generation of Th1, Th2, and Th17 cells (Figure S2C) were largely unaffected.

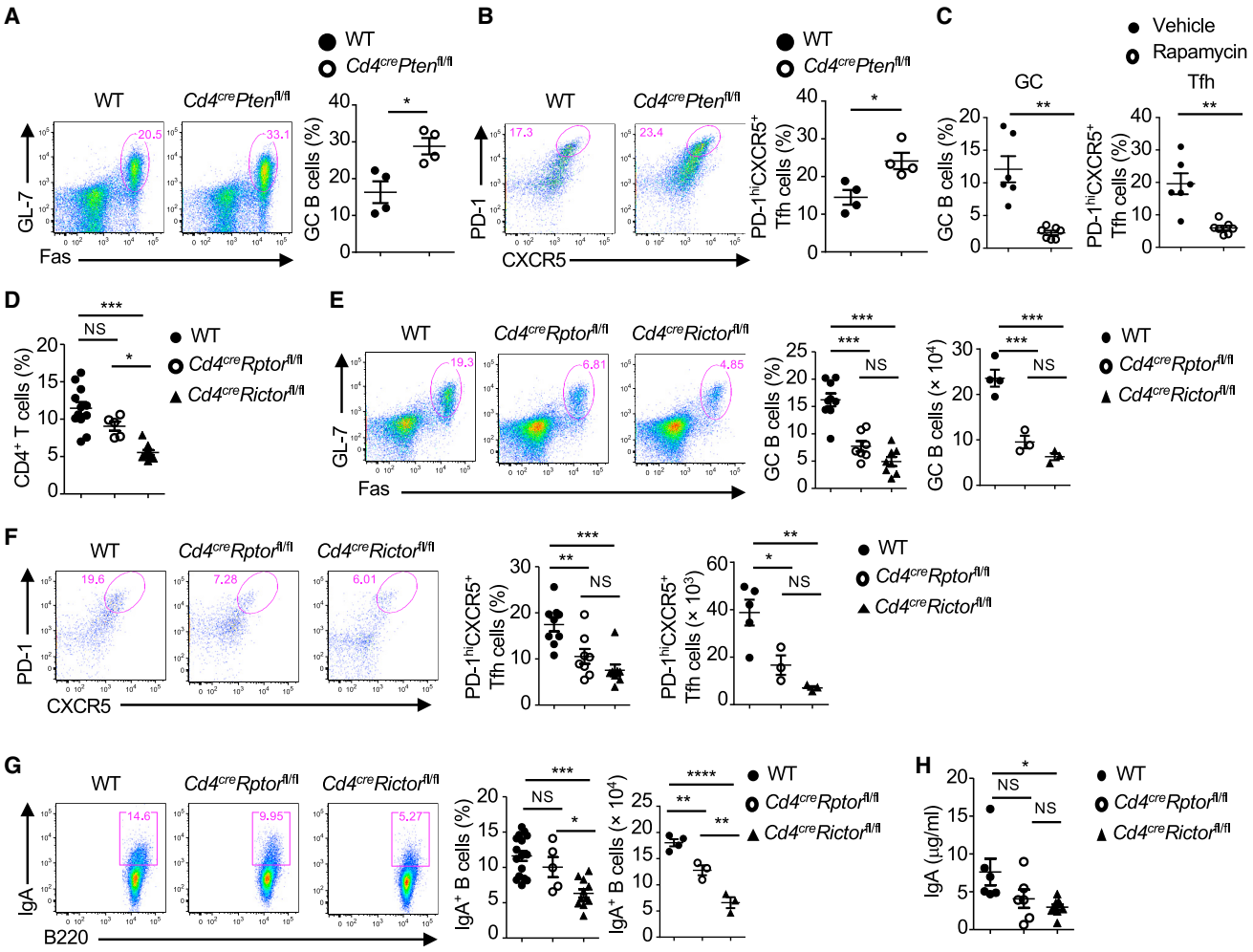

Figure 1. T Cell-Specific Loss of PTEN, Raptor, or Rictor Affects GC Formation, Tfh Cell Differentiation and IgA Production in PPs

(A and B) Flow cytometry of GC B cells (GL-7$^+$Fas$^+$) among B220$^+$ cells (A) and Tfh cells (PD-1^{hi}CXCR5$^+$) among B220$^-$CD4$^+$TCRβ$^+$ cells (B) in PPs from WT and *Cd4*^{cre}*Pten*$^{fl/fl}$ mice. Right shows the frequency of GC B cells or Tfh cells.

(C) Frequencies of GC B cells and Tfh cells in PPs from mice treated with vehicle or rapamycin.

(D) Frequency of CD4$^+$ T cells in PPs from WT, *Cd4*^{cre}*Rptor*$^{fl/fl}$, and *Cd4*^{cre}*Rictor*$^{fl/fl}$ mice.

(E and F) Flow cytometry of GC B cells (E) and Tfh cells (F) in PPs from WT, *Cd4*^{cre}*Rptor*$^{fl/fl}$ and *Cd4*^{cre}*Rictor*$^{fl/fl}$ mice. Right shows the frequency and number of GC B cells or Tfh cells.

(G) Flow cytometry of IgA$^+$ B cells in PPs from WT, *Cd4*^{cre}*Rptor*$^{fl/fl}$, and *Cd4*^{ce}*Rictor*$^{fl/fl}$ mice. Right shows the frequency and number of IgA$^+$ B cells.

(H) IgA concentration in fecal extracts. NS, not significant; *p < 0.05, **p < 0.01, ***p < 0.001, ****p < 0.0001 (one-way ANOVA, D–H; Mann-Whitney test, A–C). Data are pooled from two (C and H) or representative of three (A, B, D–G) independent experiments. Error bars represent SEM. See also Figure S1.

To determine whether these Tfh cell defects are cell intrinsic, we constructed mixed bone marrow (BM) chimeras by reconstituting lethally irradiated TCR-β and TCR-δ double-deficient (*Tcrb*$^{-/-}$*Tcrd*$^{-/-}$) mice with BM cells from CD45.1$^+$ mice, together with those from WT, OX40^{cre}*Rptor*$^{fl/fl}$ or OX40^{cre}*Rictor*$^{fl/fl}$ mice. T cells derived from either Raptor- or Rictor-deficient donors had severely defective Tfh cells in PPs (Figure 2F). Hence, impaired Tfh cell differentiation in the absence of Raptor or Rictor is a cell-intrinsic defect.

Similar to *Cd4*^{cre}*Rictor*$^{fl/fl}$ mice (Figure 1D), OX40^{cre}*Rictor*$^{fl/fl}$ mice had a reduced frequency and number of CD4$^+$ T cells in PPs (Figure 2G and Figure S2D). This defect was not evident in spleen or mesenteric lymph nodes (Figure 2G), suggesting a possible defect in T cell distribution. Indeed, examination of CD3 immunohistochemistry revealed a significant reduction of T cells within GCs in OX40^{cre}*Rictor*$^{fl/fl}$ mice, but not in OX40^{cre}*Rptor*$^{fl/fl}$ mice (Figure 2H). Furthermore, B cells in PPs from OX40^{cre}*Rictor*$^{fl/fl}$ mice exhibited a strongly reduced IgA expression, and those from OX40^{cre}*Rptor*$^{fl/fl}$ mice were diminished as well, albeit to a lesser degree (Figure 2I). Of note, we found a modest reduction of Tfr cells in OX40^{cre}*Rictor*$^{fl/fl}$ mice (Figure S2E); however, because Treg-specific deletion of Rictor did not affect Tfh or GC cells in PPs (Figure S1G), Tfr cells seemed unlikely to cause defective Tfh cell differentiation. These data demonstrate that mTORC1 and mTORC2 promote spontaneous Tfh cell differentiation, GC formation, and IgA production in PPs in a cell-intrinsic manner and mTORC2 promotes proper T cell localization within PPs.

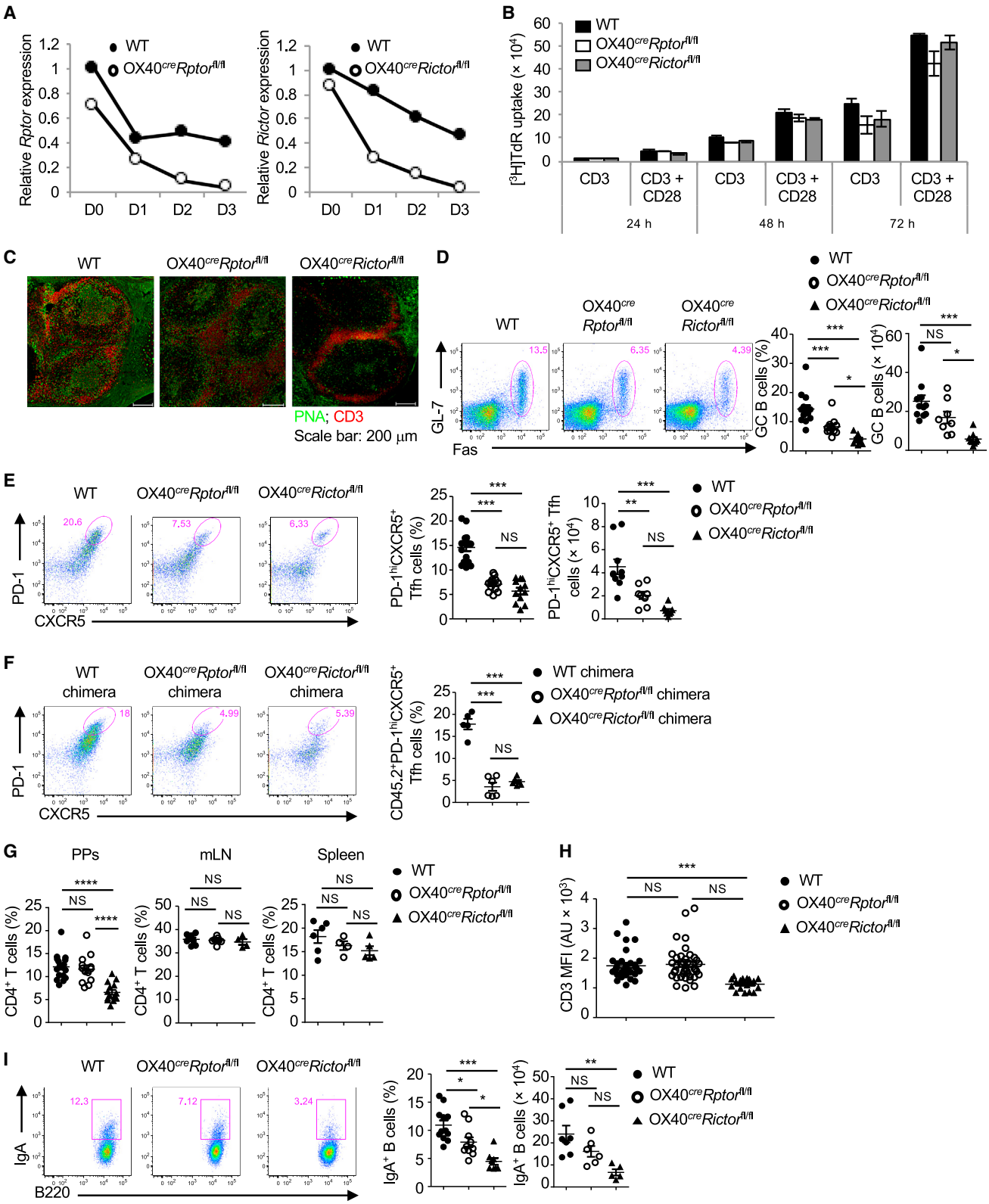

Figure 2. Deletion of Raptor and Rictor via OX40-Cre Impairs Tfh Cell Differentiation and Immune Homeostasis in PPs

(A) RNA analysis of *Rptor* and *Rictor* in freshly isolated or activated T cells from WT, OX40^{cre}*Rptor*$^{fl/fl}$, or OX40^{cre}*Rictor*$^{fl/fl}$ mice.

(B) Naive T cells from WT, OX40^{cre}*Rptor*$^{fl/fl}$, and OX40^{cre}*Rictor*$^{fl/fl}$ mice were stimulated with anti-CD3 alone or anti-CD3 plus anti-CD28 for different days, followed by [^{3}H]-thymidine incorporation analysis.

(legend continued on next page)

mTORC2 Signaling Promotes Tfh Cell Responses through Inhibition of Foxo1

We examined the role of mTORC2 in the regulation of molecules involved in T cell homeostasis. $CD4^+$ T cells in PPs of $OX40^{cre}Rictor^{fl/fl}$ mice exhibited increased CD62L, CD127 (IL-7Rα), and CCR7 and reduced CD69 expression (Figure 3A). These molecules are known to be under the control of Foxo1 (Kerdiles et al., 2009; Ouyang et al., 2009). Considering the requirement of Rictor in $CD4^+$ T cell abundance in PPs selectively (Figure 2G), we asked whether T cells from different lymphoid tissues exhibit differential expression of Foxo1-dependent targets. MP $CD4^+$ T cells from PPs showed highest expression of CD69, but lowest expression of CD127, CCR7, and CD62L (Figure 3B), as well as *S1pr1* and *Klf2*, also targets of Foxo1 (Figure 3C). Thus, MP T cells from PPs have reduced Foxo1-dependent gene expression compared to those from peripheral lymphoid organs.

Foxo1 is a key negative regulator for Tfh cell differentiation (Stone et al., 2015; Xiao et al., 2014). Akt phosphorylates Foxo proteins, leading to their nuclear export and degradation (Hedrick et al., 2012), but it remains unknown whether Foxo proteins functionally interplay with mTOR in $CD4^+$ T cells. We therefore examined subcellular localization of Foxo1 in activated T cells from $OX40^{cre}Rptor^{fl/fl}$ and $OX40^{cre}Rictor^{fl/fl}$ mice. Anti-ICOS stimulation triggered robust Foxo1 nuclear export in WT and Raptor-deficient T cells, but not in Rictor-deficient T cells (Figure 3D). These results indicate that ICOS affects Foxo1 activity in T cells through mTORC2.

We next determined whether ablation of Foxo1 could restore defective Tfh cells in Rictor-deficient mice. Due to development of autoimmunity in $OX40^{cre}Foxo1^{fl/fl}$ mice (probably due to Treg cell defects [Ouyang et al., 2012]), we used the $Cd4^{cre}$ system to generate compound mutant mice. Inactivation of Foxo1 in T cells largely restored Tfh and GC B cells in $Cd4^{cre}Rictor^{fl/fl}Foxo1^{fl/fl}$ mice (Figures S3A and S3B). Given the disrupted T cell homeostasis in $Cd4^{cre}Foxo1^{fl/fl}$ mice (Kerdiles et al., 2009; Kerdiles et al., 2010; Ouyang et al., 2009; Ouyang et al., 2010), we also examined whether a partial loss of Foxo1 could ameliorate the Tfh defect. The reduced Tfh and GC cell responses in $Cd4^{cre}Rictor^{fl/fl}$ mice were significantly restored in $Cd4^{cre}Rictor^{fl/fl}Foxo1^{fl/+}$ mice, albeit to a partial degree (Figures 3E and 3F). Therefore, Foxo1 activity was upregulated in the absence of mTORC2, and reduction of Foxo1 activity partially restored defective Tfh cells.

mTORC1 and mTORC2 Orchestrate Overlapping and Discrete Gene-Expression Programs

To further explore how mTORC1 and mTORC2 control T cell homeostasis and Tfh cell differentiation, we compared gene-expression profiles of MP T cells from PPs of $Cd4^{cre}Rptor^{fl/fl}$ and $Cd4^{cre}Rictor^{fl/fl}$ mice (*Cd4*-Cre was used to ensure efficient deletion). The differentially expressed genes from Raptor or Rictor-deficient T cells (with greater than 0.5 $\log_2$ fold change compared to WT) corresponded to 1,802 probes. Among them, 209 probes (R1) were concordantly changed, while 45 probes (R3) showed opposite direction of changes between the two mutant cells (Figure 3G). More probes, however, showed altered expression in only one of the mutant cells, with 1,093 probes in Raptor-deficient (R4) and 455 probes in Rictor-deficient cells (R2) (Figure 3G). A heatmap of differentially expressed genes showed that Raptor and Rictor control both overlapping and distinct gene-expression profiles (Figure S3C).

We performed gene-set enrichment analysis (GSEA) to compare gene expression of Raptor or Rictor-deficient T cells versus WT cells. This unbiased approach identified a number of downregulated pathways in both Raptor and Rictor-deficient T cells, including cell cycle, pyruvate metabolism and citric acid TCA cycle, glucose metabolism, and lipid metabolism (Figure S3D). In contrast, cholesterol biosynthesis was suppressed in Raptor-deficient cells selectively, while cytokine-cytokine receptor interaction and chemokine-chemokine receptor pathways were upregulated in the absence of Rictor, but not Raptor (Figure S3D). When applying GSEA to curate the transcriptional signatures of Tfh cells (Choi et al., 2015; Yusuf et al., 2010), we found inhibition of Tfh cell gene signatures in Raptor and Rictor-deficient cells (Figure 3H). There was little overlap between Raptor and Rictor-dependent Tfh cell signatures, suggesting that mTORC1 and mTORC2 mediate discrete programs of Tfh cell differentiation (Figure 3H). This was further supported by ingenuity pathway analysis (IPA) that revealed activation of immune cell trafficking in the absence of Rictor but not Raptor (Figure S3E). Thus mTORC1 and mTORC2 orchestrate both overlapping and distinct gene-expression programs in cell metabolism, immune functions, and Tfh cell differentiation.

mTORC1 and mTORC2 Are Essential for Tfh Cell Induction upon LCMV Infection

We next explored the roles of mTOR in Tfh cell differentiation in peripheral immune tissues. Under steady state, the spleen from WT, $OX40^{cre}Rptor^{fl/fl}$, or $OX40^{cre}Rictor^{fl/fl}$ mice showed no differences in GC B cells (Figure S4A) or Tfh cells (Figure S4B). To examine GC reaction in response to acute viral infection, we challenged mice with LCMV Armstrong strain. At day 8 after infection, GC B cells were reduced in both $OX40^{cre}Rptor^{fl/fl}$ and $OX40^{cre}Rictor^{fl/fl}$ mice (Figures 4A and 4B). Furthermore, IgD^-CD138^+ plasma B cells were significantly reduced in $OX40^{cre}Rptor^{fl/fl}$ mice and, to a lesser degree, $OX40^{cre}Rictor^{fl/fl}$

(C) Immunohistochemistry of GCs in PPs of WT, $OX40^{cre}Rptor^{fl/fl}$, and $OX40^{cre}Rictor^{fl/fl}$ mice. Scale bars represent 200 μm.
(D and E) Flow cytometry of GC B cells (D) and Tfh cells (E) in PPs of WT, $OX40^{cre}Rptor^{fl/fl}$, and $OX40^{cre}Rictor^{fl/fl}$ mice. Right shows the frequency and number of GC B cells or Tfh cells.
(F) Flow cytometry of Tfh cells among $CD45.2^+B220^-CD4^+TCR\beta^+$ cells in PPs from mixed BM chimeras constructed by mixing BM cells from WT, $OX40^{cre}Rptor^{fl/fl}$, or $OX40^{cre}Rictor^{fl/fl}$ mice and $CD45.1^+$ mice and injecting into $Tcrb^{-/-}Tcrd^{-/-}$ recipient mice. Right shows the frequency of Tfh cells.
(G) Frequencies of $CD4^+$ T cells in PPs, mesenteric lymph nodes (mLN) and spleen from WT, $OX40^{cre}Rptor^{fl/fl}$ and $OX40^{cre}Rictor^{fl/fl}$ mice.
(H) Quantification of anti-CD3 mean fluorescence intensity (MFI) within GCs in PPs based on the immunohistochemistry images in (C).
(I) Flow cytometry of IgA^+ B cells in PPs from WT, $OX40^{cre}Rptor^{fl/fl}$, and $OX40^{cre}Rictor^{fl/fl}$ mice. Right shows the frequency and number of IgA^+ B cells. NS, not significant; $^*p < 0.05$, $^{**}p < 0.01$, $^{***}p < 0.001$ (one-way ANOVA). Data are representative of two (A and B) or at least three (C–I) independent experiments. Error bars represent SEM. See also Figure S2.

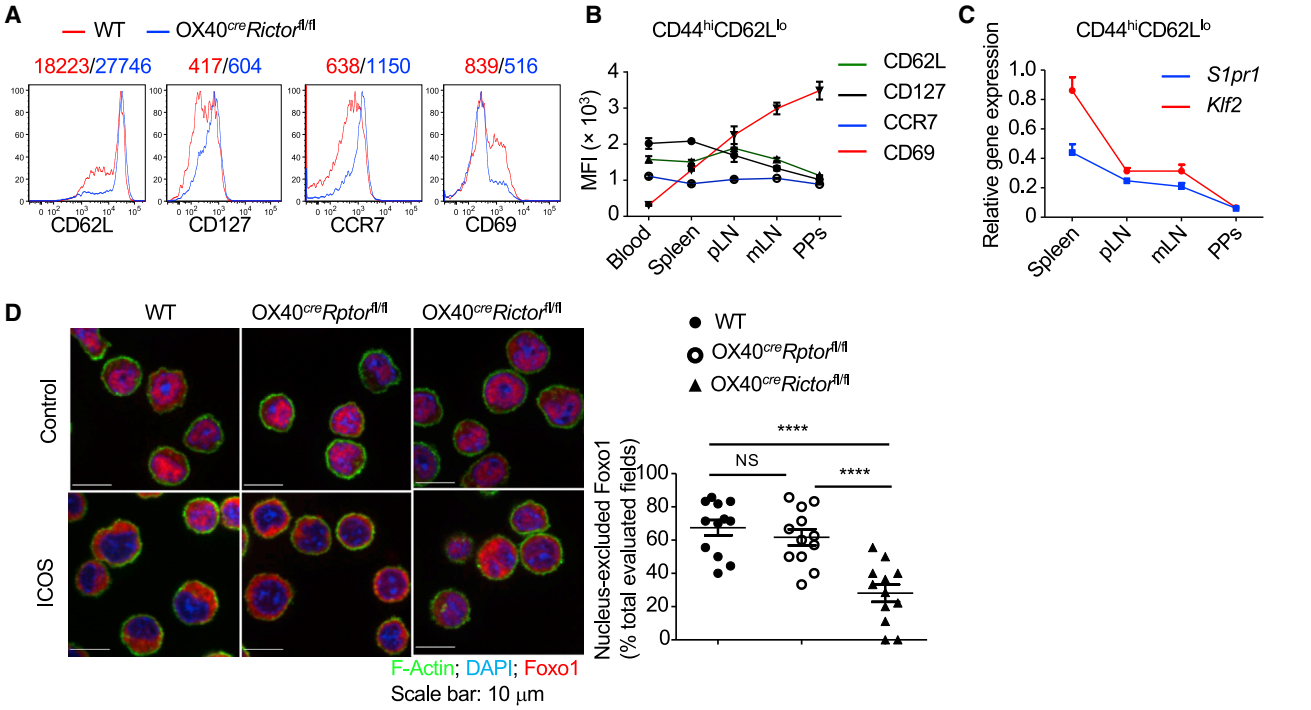

(legend on next page)

mice (Figures 4C and 4D). Examination of Tfh cell markers PD-1 and CXCR5 (Figures 4E and 4F) or Bcl6 and CXCR5 (Figures S4C and S4D) revealed a significant reduction of Tfh cells in both OX40^{cre}*Rptor*$^{fl/fl}$ and OX40^{cre}*Rictor*$^{fl/fl}$ mice. To investigate whether these defects were cell-intrinsic, we constructed mixed BM chimeras by reconstituting sub-lethally irradiated *Rag1*$^{-/-}$ mice with BM cells from CD45.1^{+} mice, together with those from WT, OX40^{cre}*Rptor*$^{fl/fl}$ or OX40^{cre}*Rictor*$^{fl/fl}$ mice. At 2 months after reconstitution, we infected chimeras with LCMV. While T cells derived from CD45.1^{+} BM cells had normal Tfh cell differentiation (Figures 4G and 4H, right panels), T cells from OX40^{cre}*Rptor*$^{fl/fl}$ or OX40^{cre}*Rictor*$^{fl/fl}$ BM cells had reduced Tfh cells relative to WT cells (Figures 4G and 4H, left panels). Given the shared developmental history between Tfh and Th1 cells (Nakayamada et al., 2011), we investigated LCMV-induced Th1 cell differentiation. Raptor deficiency reduced Th1 cells (T-bet^{+}CXCR5^{lo}) (Figure S4E), while Rictor deficiency slightly elevated Th1 cells (Figure S4F). Therefore, both mTORC1 and mTORC2 are required for Tfh and GC B cell responses upon viral infection, whereas mTORC1 but not mTORC2 contributes to Th1 cell differentiation.

mTORC1 and mTORC2 Promote Foreign Antigen-Induced Tfh Cell Responses

To further assess the role of mTORC1 and mTORC2 in GC responses, we immunized mice with ovalbumin linked to 4-hydroxy-3-nitrophenylacetyl hapten (NP-OVA) (Shrestha et al., 2015). Both OX40^{cre}*Rptor*$^{fl/fl}$ and OX40^{cre}*Rictor*$^{fl/fl}$ mice had reduced GC B cells in the spleen (Figures 5A and 5B) and draining lymph nodes (data not shown). Confocal microscopic analysis revealed smaller size of GCs (Figure 5C), and analysis of serum antibodies showed reduction of anti-NP IgM and IgG, and IgG subtypes IgG1, IgG2c, and IgG3 titers (Figure 5D). OX40^{cre}*Rptor*$^{fl/fl}$ and OX40^{cre}*Rictor*$^{fl/fl}$ mice also had markedly reduced Tfh cells, as revealed by co-expressed markers PD-1 and CXCR5 (Figures 5E and 5F), ICOS and CXCR5 (Figure S5A), or Bcl6 and CXCR5 (Figure S5B). Altogether, mTORC1 and mTORC2 are required for Tfh cell differentiation, GC formation, and humoral responses after foreign antigen immunization.

To test whether the requirements of mTORC1 and mTORC2 in Tfh cell differentiation are cell-autonomous, we immunized mixed BM chimeras (as described in Figures 4G and 4H) with NP-OVA. T cells derived from OX40^{cre}*Rptor*$^{fl/fl}$ or OX40^{cre}*Rictor*$^{fl/fl}$ BM cells had diminished Tfh cell generation (Figures 5G and 5H). Moreover, to exclude altered TCR repertoire as a potential contributing factor, we bred OX40^{cre}*Rptor*$^{fl/fl}$ and OX40^{cre}*Rictor*$^{fl/fl}$ mice with OT-II transgenic mice expressing OVA-specific TCRs. We transferred naive T cells from these mice into CD45.1^{+} recipients and immunized them with NP-OVA. Compared with WT OT-II T cells, those deficient in Raptor or Rictor generated significantly reduced Tfh cells (Figure 5I). Collectively, mTORC1 and mTORC2 are required for Tfh cell differentiation after immunization via T cell-intrinsic and antigen-specific mechanisms.

Raptor or Rictor Deficiency Impairs ICOS-Induced Signaling and Metabolism

We determined upstream and downstream pathways mediated by mTORC1 and mTORC2 for Tfh cell differentiation. Expression of Tfh cell-associated transcription factors Bcl6 and IRF4 (Bollig et al., 2012) was undisturbed by Raptor or Rictor deficiency (Figure 6A). ICOS, which regulates late-stage Tfh cell differentiation via Foxo1 (Stone et al., 2015; Weber et al., 2015), was modestly reduced in the absence of Raptor, but not Rictor, in the spleen after immunization or PPs under steady state (Figure 6B). Because mTORC2 mediates ICOS-induced Foxo1 nuclear exclusion (Figure 3D), we examined expression of Foxo1-dependent target genes in splenic Tfh cells after NP-OVA immunization. Rictor-deficient Tfh cells expressed higher amounts of Foxo1 target genes, including *Klf2*, *Il7r*, and *Ccr7* (Figure 6C). Flow cytometry analysis revealed increased expression of CD62L and CD127 and reduced expression of CD69 (Figure 6D). Altogether, loss of Raptor modestly reduces ICOS expression, whereas Rictor deficiency upregulates Foxo1 gene targets.

To examine ICOS-induced signaling events, we stimulated T cell blasts from OX40^{cre}*Rptor*$^{fl/fl}$ and OX40^{cre}*Rictor*$^{fl/fl}$ mice with anti-ICOS, which induced phosphorylation of S6 and Akt (serine 473) that are the respective targets of mTORC1 and mTORC2. These phosphorylation events were profoundly lost in the absence of Raptor and Rictor, respectively (Figure 6E). Compared to anti-CD3 stimulation alone, anti-CD3 plus anti-ICOS promoted cell lipogenesis (Figures 6F and 6G) and glycolysis (Figure 6H), but such enhancement was blunted by deficiency of Raptor or Rictor (Figures 6F–6H). Moreover, defective glucose uptake was evident in vivo in Tfh cells from immunized

Figure 3. mTORC2 Promotes Tfh Cell Differentiation in PPs by Suppressing Foxo1 Activity

(A) Flow cytometry of CD62L, CD127, CCR7, and CD69 expression on CD4^{+} T cells in PPs from WT and OX40^{cre}*Rictor*$^{fl/fl}$ mice.

(B) MFI of CD62L, CD127, CCR7, and CD69 on memory-phenotype (CD44^{hi}CD62L^{lo}) T cells from blood, spleen, peripheral lymph nodes (pLN), mesenteric lymph nodes (mLN), and PPs.

(C) RNA analysis of *S1pr1* and *Klf2* expression in CD44^{hi}CD62L^{lo} T cells.

(D) Confocal microscopy imaging of Foxo1 nuclear exclusion. Activated T cells were rested and re-stimulated with anti-ICOS antibody and then fixed and stained with anti-F-Actin, anti-Foxo1, and DAPI. Right shows calculated percentages of cells with Foxo1 excluded from the nucleus.

(E and F) Flow cytometry of Tfh cells (E) and GC B cells (F) in PPs of WT, *Cd4*^{cre}*Rictor*$^{fl/fl}$, and *Cd4*^{cre}*Rictor*$^{fl/fl}$*Foxo1*$^{fl/+}$ mice. Right shows the frequency and number of Tfh cells or GC B cells.

(G) Comparison of gene-expression changes between WT and *Cd4*^{cre}*Rptor*$^{fl/fl}$ versus WT and *Cd4*^{cre}*Rictor*$^{fl/fl}$ memory phenotype (MP) T cells. Genes with altered expression (with > 0.5 $\log_2$ fold change) in either *Cd4*^{cre}*Rptor*$^{fl/fl}$ or *Cd4*^{cre}*Rictor*$^{fl/fl}$ mice were clustered into four groups. R1, concordant expression between *Cd4*^{cre}*Rptor*$^{fl/fl}$ and *Cd4*^{cre}*Rictor*$^{fl/fl}$ cells; R2, selectively altered in *Cd4*^{cre}*Rictor*$^{fl/fl}$ cells; R3, discordant expression between *Cd4*^{cre}*Rptor*$^{fl/fl}$ and *Cd4*^{cre}*Rictor*$^{fl/fl}$ cells; and R4, selectively altered in *Cd4*^{cre}*Rptor*$^{fl/fl}$ cells.

(H) GSEA of the Tfh cell gene signature in *Cd4*^{cre}*Rptor*$^{fl/fl}$ (left) and *Cd4*^{cre}*Rictor*$^{fl/fl}$ (right) MP T cells relative to the expression in WT MP T cells. The heatmaps on the left of GSEA plots show the top hit (leading-edge) genes. NS, not significant; **p < 0.01, ***p < 0.001, ****p < 0.0001 (one-way ANOVA). Data are representative of at least three (A, E, F), 2 (B–D) and one (G and H; n = 5 mice for WT mice, three mice for *Cd4*^{cre}*Rptor*$^{fl/fl}$ mice, and four for *Cd4*^{cre}*Rictor*$^{fl/fl}$ mice) independent experiments. Error bars represent SEM. See also Figure S3.

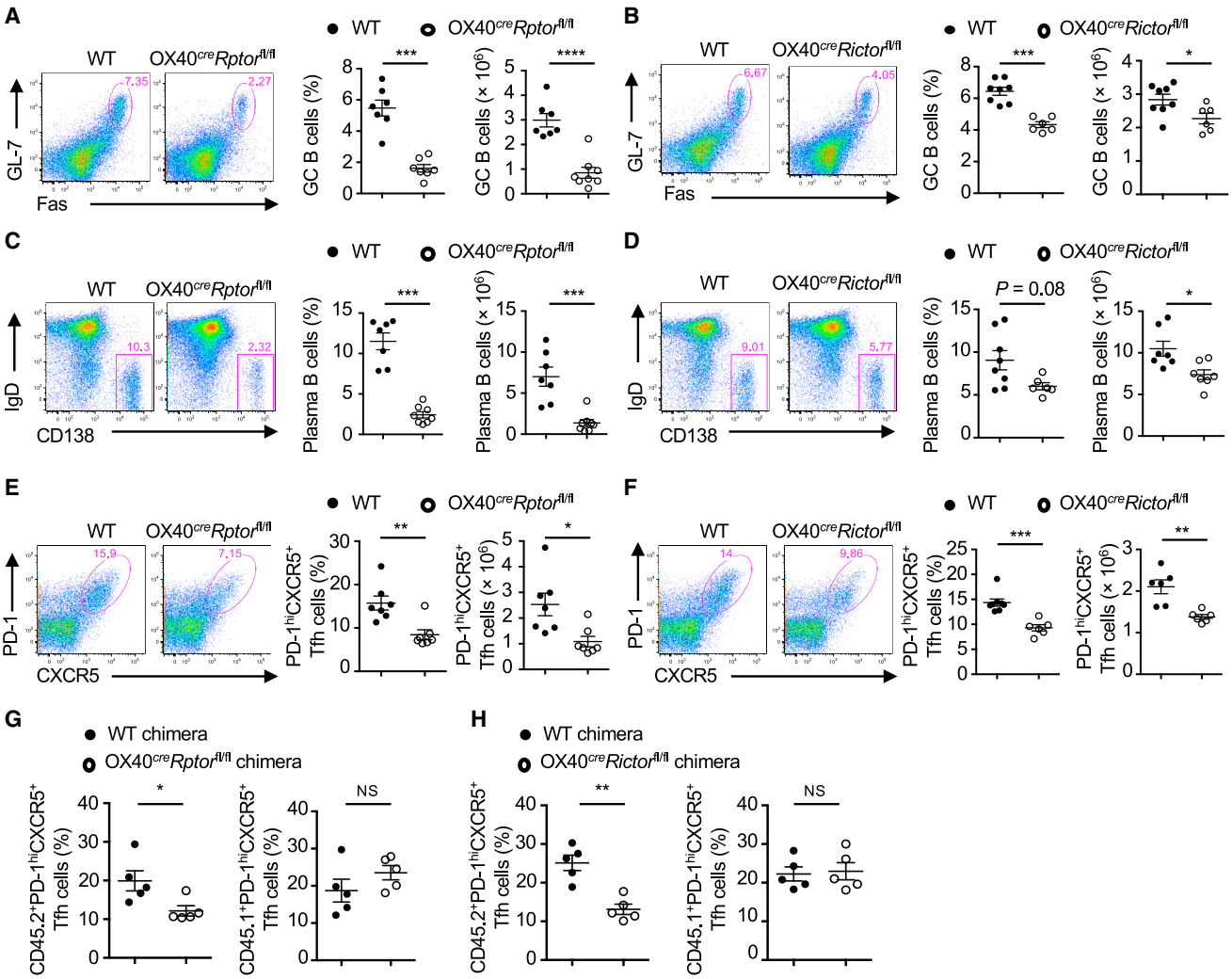

Figure 4. mTORC1 and mTORC2 Promote Tfh Cell and GC Responses after LCMV Infection

(A and B) Flow cytometry of GC B cells in the spleen from WT and OX40^{cre}*Rptor*$^{fl/fl}$ mice (A) or OX40^{cre}*Rictor*$^{fl/fl}$ mice (B) at 8 days after challenge with LCMV Armstrong strain. Right shows the frequency and number of GC B cells.

(C and D) Flow cytometry of IgD^{-}CD138^{+} plasma B cells in the spleen from WT and OX40^{cre}*Rptor*$^{fl/fl}$ mice (C) or OX40^{cre}*Rictor*$^{fl/fl}$ mice (D) at 8 days after LCMV infection. Right shows the frequency and number of plasma B cells.

(E and F) Flow cytometry of Tfh cells in the spleen from WT and OX40^{cre}*Rptor*$^{fl/fl}$ mice (E) or OX40^{cre}*Rictor*$^{fl/fl}$ mice (F) at 8 days after LCMV infection. Results are gated on B220^{-}CD4^{+}TCRβ^{+} cells. Right shows the frequency and number of Tfh cells.

(G and H) The percentages of Tfh cells among CD45.2^{+}B220^{-}CD4^{+}TCRβ^{+} donor-derived cells (left) or CD45.1^{+}B220^{-}CD4^{+}TCRβ^{+} cells (right) in the spleen from mixed BM chimeras at 8 days after LCMV infection; chimeras were reconstituted with BM cells from CD45.1^{+} mice and WT, OX40^{cre}*Rptor*$^{fl/fl}$ mice (G) or OX40^{cre}*Rictor*$^{fl/fl}$ mice (H). *$p < 0.05$, **$p < 0.01$, ***$p < 0.001$, ****$p < 0.0001$ (Mann-Whitney test for frequencies, unpaired Student's t test for numbers). Results were pooled from 2 (A, C, and E) or represent 2 (B, D, F, G, and H) independent experiments. Error bars represent SEM. See also Figure S4.

OX40^{cre}*Rptor*$^{fl/fl}$ and OX40^{cre}*Rictor*$^{fl/fl}$ mice, as indicated by staining with the glucose analog, 2-(*N*-(7-Nitrobenz-2-oxa-1,3-diazol-4-yl)Amino)-2-Deoxyglucose (2-NBDG) (Figure 6I). Finally, we transferred naive OT-II T cells to recipient mice, and NP-OVA immunization activated all donor T cells by day 5, as indicated by the uniformly high CD44 expression (Figure S6A). We compared Tfh cells to non-Tfh cells (Figure S6B) in terms of cell size, 2-NBDG staining, CD71 and CD98 expression (Figure S6C), and expression of key glycolytic genes (Figure S6D). In all cases, Tfh cells exhibited higher metabolic activities. Therefore, mTORC1 and mTORC2 link ICOS stimulation to metabolic activities.

The proto-oncogene Myc mediates metabolic reprogramming of T cells responding to antigen stimulation (Wang et al., 2011). To test whether Myc was important for Tfh cell differentiation, we generated OX40^{cre}*Myc*$^{fl/fl}$ mice. OX40^{cre}*Myc*$^{fl/fl}$ mice showed a profound reduction of GC and Tfh cells following antigen stimulation (Figure 6J), as well as in PPs under steady state (Figure 6K). Thus, Myc function is required for Tfh cell differentiation.

Glucose Metabolism Regulates Tfh Cell Differentiation

We next directly tested the metabolic requirements of Tfh cells. To this end, we differentiated naive CD4 T cells in vitro to

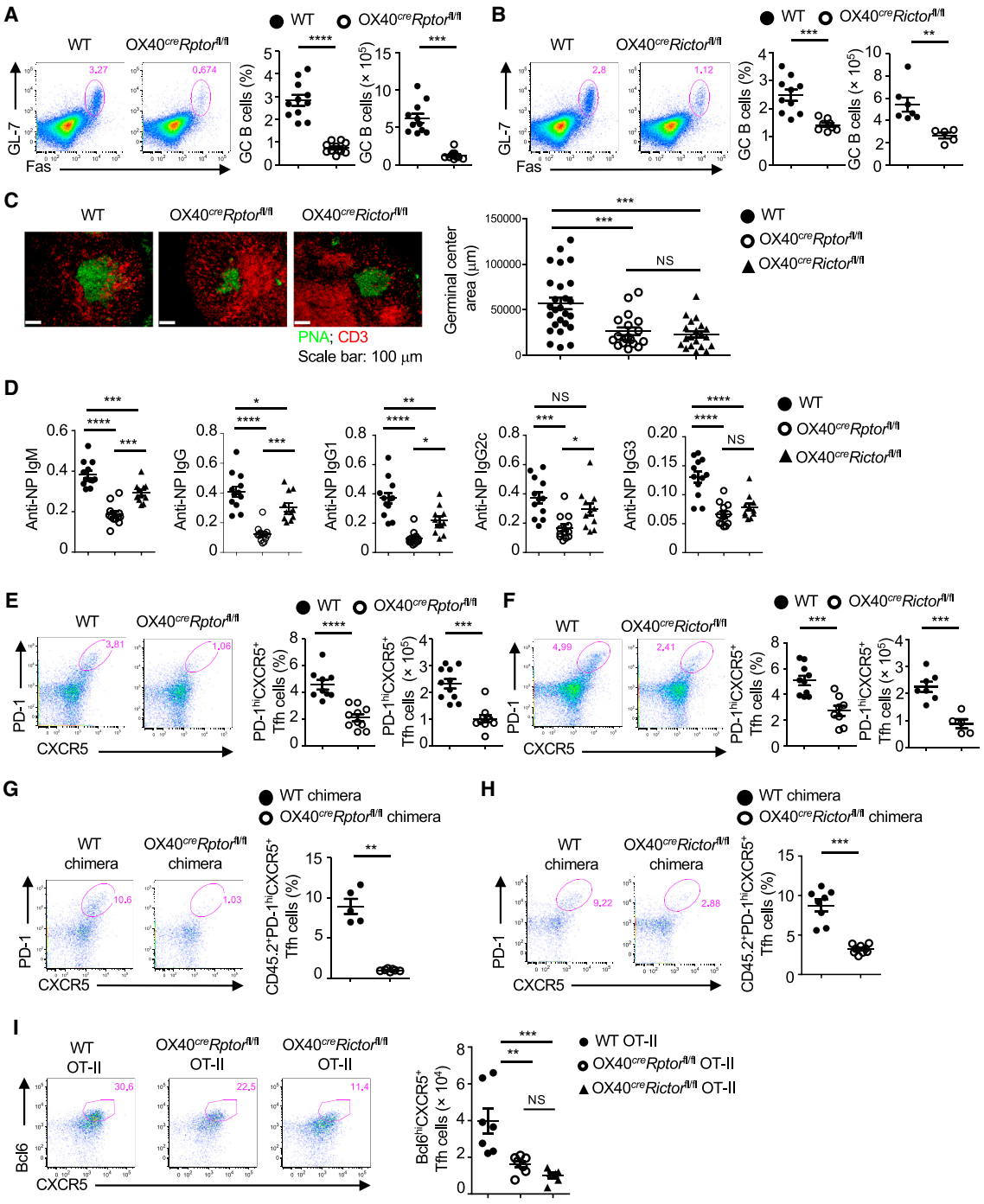

Figure 5. OX40^{cre}*Rptor*$^{fl/fl}$ and OX40^{cre}*Rictor*$^{fl/fl}$ Mice Fail to Mount Efficient GC Reaction after Immunization via Cell-Intrinsic and Antigen-Specific Mechanisms

(A and B) Flow cytometry of GC B cells in spleen from WT and OX40^{cre}*Rptor*$^{fl/fl}$ mice (A) or OX40^{cre}*Rictor*$^{fl/fl}$ mice (B) at 7 days after intraperitoneal immunization of mice with NP-OVA plus LPS in alum. Right shows the frequency and number of GC B cells. **p < 0.01, ***p < 0.001, ****p < 0.0001 (Mann-Whitney test).

(C) Immunohistochemistry of GCs in the mesenteric lymph nodes of WT, OX40^{cre}*Rptor*$^{fl/fl}$ and OX40^{cre}*Rictor*$^{fl/fl}$ mice at 7 days after immunization. Scale bars show 100 μm. Right shows calculated GC size.

(D) Measurements of anti-NP immunoglobulins in serum from immunized mice, presented as absorbance at 450 nm (A_{450}) in ELISA.

(E and F) Flow cytometry of Tfh cells in spleen from WT and OX40^{cre}*Rptor*$^{fl/fl}$ mice (E) or OX40^{cre}*Rictor*$^{fl/fl}$ mice (F) at 7 days after intraperitoneal immunization of mice with NP-OVA plus LPS in alum. Right shows the frequency and number of Tfh cells.

(legend continued on next page)

generate Tfh-like cells (Awe et al., 2015), which expressed IL-21, Bcl6, CXCR5, PD-1, and ICOS (Figures S7A–S7C). Metabolite profiles were generated using high-resolution mass spectrometry to compare the metabolome of Tfh-like cells with that of activated T cells (Tact) and Th1 and Th17 cells. Each subset was metabolically distinct (Figures 7A and 7B). Pathway analyses of altered metabolites showed that amino acid, amino sugar metabolism, and glycolytic intermediates trended higher in Tfh-like cells, but Tfh-like cells had lower amount of TCA metabolites and intermediates in cysteine and glycerophospholipid metabolism (Table S1). Consistent with Tfh cell reliance on both glucose and mitochondrial metabolism pathways, treatment of in vitro differentiated Tfh-like cells with low doses of either glycolysis inhibitor 2-deoxyglucose (2-DG) or electron transport inhibitor rotenone led to reduced number of IL-21-producing $CD4^+$ T cells (Figure 7C).

Our data show that mTOR signaling promotes glucose metabolism and uptake in Tfh cells in vivo. Indeed, in vitro induced Tfh-like cells expressed elevated Glut1 (Figures 7D and 7E). Likewise, Glut1 expression was higher on Tfh cells relatively to other non-Tfh $CD4^+$ T cells from PPs (Figure 7F) and spleens (Figure S7D). Glut1 expression was partly dependent on mTORC1 signaling, as rapamycin treatment reduced Glut1 expression in vitro (Figure S7E and S7F). Consistent with this finding, Glut1 expression was reduced in Raptor-deficient, but not Rictor-deficient, Tfh cells after LCMV infection (Figure S7G). Rapamycin treatment also suppressed glucose uptake (Figure S7H) of in vitro Tfh-like cells. T cells with transgenic expression of Glut1 (*Slc2a1*-Tg), however, were able to maintain elevated glucose uptake even when treated with rapamycin (Figure S7H). Short-term treatment with rapamycin did not affect IL-21 expression in *Slc2a1*-Tg T cells, while it suppressed IL-21 expression in WT T cells (Figure 7G). Long-term treatment of rapamycin reduced IL-21 expression in both WT and *Slc2a1*-Tg T cells, but the latter still showed increased resistance to rapamycin (Figure S7I).

The role of glucose uptake in Tfh cell differentiation was next tested by directly modulating Glut1 expression. While no difference in Tfh cell responses was observed in mice with T cell-specific deletion of Glut1 ($Cd4^{cre}Slc2a1^{fl/fl}$) after immunization with sheep red blood cells (SRBC) (Figure S7J), this genetic modification did not alter glucose uptake in Tfh cells (Figure S7K) and instead led to compensatory upregulation of Glut3 (Figure S7L). Thus, we tested whether increased glucose uptake in *Slc2a1*-Tg mice altered Tfh cell differentiation. Relative to non-transgenic controls, GC B cells and IgA-expressing B cells were elevated in PPs from *Slc2a1*-Tg mice under steady state (Figures 7H and 7I). Examination of Tfh cell signature proteins, CXCR5, PD-1, ICOS, and Bcl6, revealed increased Tfh cells in the PPs of *Slc2a1*-Tg mice (Figure 7J and Figures S7M and S7N). Further, we immunized WT mice with KLH and analyzed Glut1 expression on Tfh cells in the draining lymph nodes. Similar to steady state, Tfh cells expressed higher Glut1 relatively to activated non-Tfh $CD4^+$ cells (Figure S7O). Moreover, Tfh cells were significantly enriched in immunized *Slc2a1*-Tg mice (Figure 7K). Thus, Glut1 promotes the generation of Tfh cells under steady state and upon foreign antigen challenge.

DISCUSSION

Despite the recent identification of specific receptors and transcription factors underlying Tfh cell differentiation (Crotty, 2014), the intracellular processes linking these events remain poorly understood. Here we identified mTORC1 and mTORC2 signaling as a key mechanism that links ICOS to anabolic metabolism and transcriptional regulation, thereby driving Tfh cell differentiation and humoral immunity. mTORC1 and mTORC2 orchestrate distinct transcriptional programs, with mTORC2 selectively affecting Foxo1 activity. Moreover, ICOS stimulation strongly upregulated glycolysis and lipid biosynthesis, and loss of either mTORC1 or mTORC2 diminished such metabolic activities. These data, together with the results from Glut1-transgenic and Myc-deficient systems that demonstrated the effects of in vivo metabolic modulation on Tfh cell responses, support the crucial roles of glucose metabolism in Tfh cell differentiation. Altogether, our study illustrates that mTORC1 and mTORC2 link immune signals to metabolic and transcriptional activities for Tfh cell differentiation.

Spontaneous Tfh cell generation maintains GC responses in PPs that contribute to mucosal IgA production (Fagarasan et al., 2010), but the underlying molecular pathways remain elusive. Our study links mTOR and cellular metabolism to Tfh cell differentiation in PPs. Whereas both mTORC1 and mTORC2 are important in this process, mTORC2 is selectively required for proper T cell localization in PPs, expression of Foxo1 targets, and nuclear exclusion of Foxo1 upon ICOS ligation. Reduced Tfh cell differentiation in Rictor-deficient mice could be partially restored by deletion of one allele of Foxo1, highlighting an ICOS-mTORC2-Foxo1 signaling axis in Tfh cell responses. Of note, whereas previous work in $CD8^+$ T cells associates mTORC1 with T cell migration (Finlay and Cantrell, 2011; Finlay et al., 2012), our results here reveal a function of mTORC2 in mediating $CD4^+$ T cell accumulation specifically in PPs. Also, in contrast to other effector T cell subsets in which mTORC1 generally plays a dominant role relative to mTORC2 (Chi, 2012), mTORC2 plays a more prominent role in Tfh cell differentiation and immune homeostasis in PPs. These findings highlight the unique signaling requirements of Tfh cells.

A recent report has found that shRNA-mediated silencing of mTOR or Raptor enhances Tfh cell frequency following

(G and H) Flow cytometry of Tfh cells ($PD\text{-}1^{hi}CXCR5^+$ in $CD45.2^+B220^-CD4^+TCR\beta^+$ donor-derived cells) in spleen from mixed BM chimeras reconstituted with BM cells from $CD45.1^+$ mice and WT or $OX40^{cre}Rptor^{fl/fl}$ (G) or $OX40^{cre}Rictor^{fl/fl}$ (H) mice at 7 days after intraperitoneal immunization of mice with NP-OVA plus LPS in alum. Right shows the frequency of Tfh cells.

(I) Naive $CD4^+$ T cells from WT OT-II, $OX40^{cre}Rptor^{fl/fl}$ OT-II or $OX40^{cre}Rictor^{fl/fl}$ OT-II mice were transferred into $CD45.1^+$ mice. The recipient mice were immunized with NP-OVA plus LPS in alum through footpad, and $Bcl6^{hi}CXCR5^+$ Tfh cells among $CD45.2^+B220^-CD4^+TCR\beta^+$ donor cells in popliteal lymph nodes were analyzed at 5 days after immunization. Right shows the number of Tfh cells. NS, not significant; $^*p < 0.05$, $^{**}p < 0.01$, $^{***}p < 0.001$, $^{****}p < 0.0001$ (one-way ANOVA). Data are pooled from three (A–F) or representative of two (G–I) independent experiments. Error bars represent SEM. See also Figure S5.

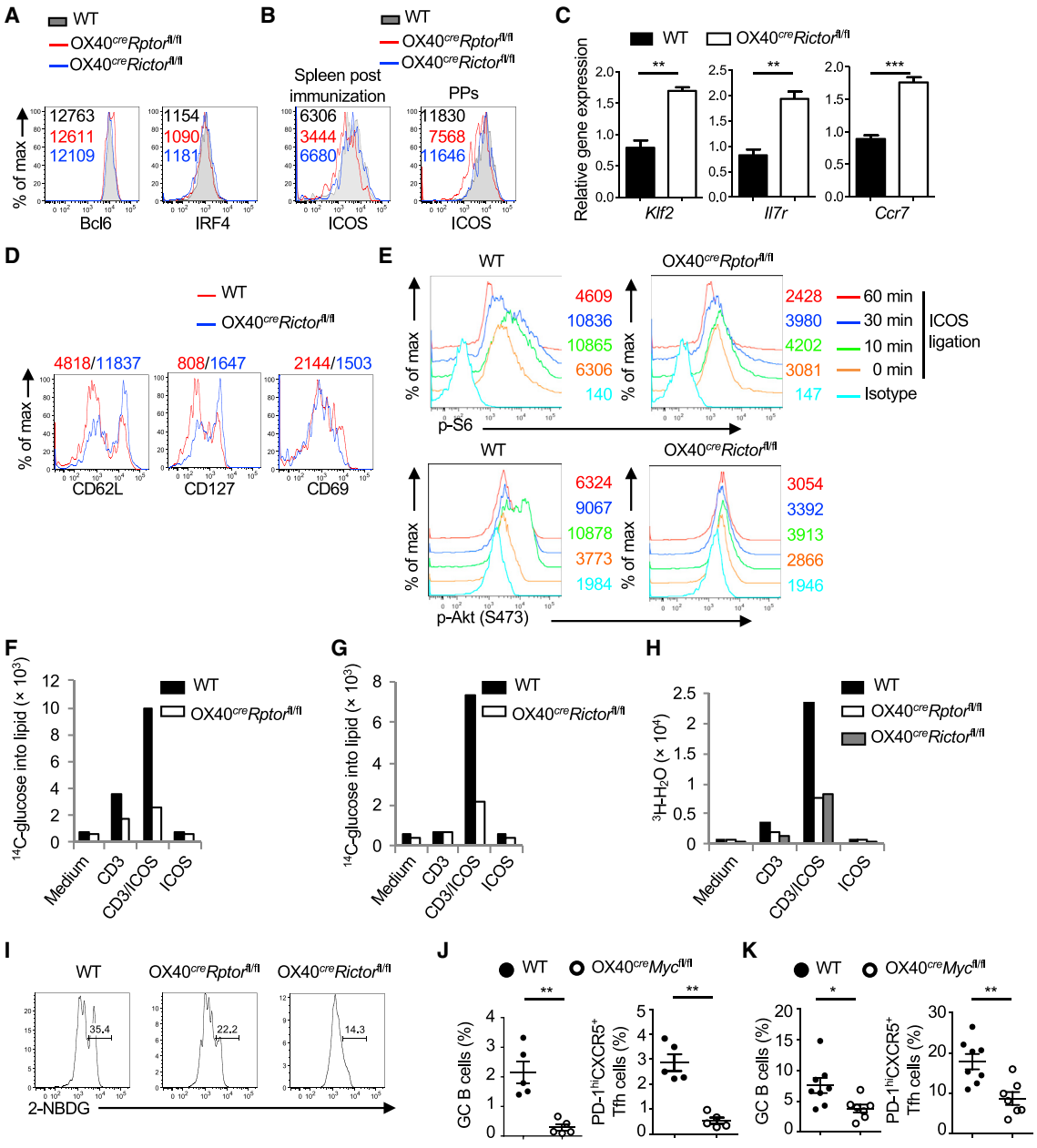

Figure 6. Raptor and Rictor Are Required for ICOS-Mediated Signaling Events and Anabolic Metabolism

(A–D) Mice were immunized by NP-OVA plus LPS in alum, and splenic Tfh cells were analyzed for the expression of Bcl6 and IRF4 (A), ICOS (B, left), *Klf2*, *Il7r* and *Ccr7* (C), and CD62L, CD127, and CD69 (D). (B, right) ICOS expression on Tfh cells from PPs under steady state.

(E) Naive CD4$^+$ T cells from WT, OX40^{cre}*Rptor*$^{fl/fl}$ or OX40^{cre}*Rictor*$^{fl/fl}$ mice were activated by anti-CD3 and anti-CD28 for 3 days, rested for 3 hr, and re-stimulated with anti-ICOS. Phosphorylation of S6 and Akt at Ser 473 was examined by flow cytometry at indicated time points.

(F–H) Metabolic assays in activated T cells that were re-stimulated with indicated stimuli for 24 hr, with the final 4 hr labeled with ^{14}C-acetate to measure de novo lipogenesis (F and G) or with [3-^{3}H]-glucose to measure glycolysis (H).

(I) Glucose uptake as measured by 2-NBDG labeling in Tfh cells in spleen from WT, OX40^{cre}*Rptor*$^{fl/fl}$, and OX40^{cre}*Rictor*$^{fl/fl}$ mice at 7 days after NP-OVA immunization.

(J) Frequencies of GC and Tfh cells in spleen from WT and OX40^{cre}*Myc*$^{fl/fl}$ mice at 7 days after NP-OVA immunization.

(K) Frequencies of GC and Tfh cells in PPs from WT and OX40^{cre}*Myc*$^{fl/fl}$ mice under steady state. *p < 0.05, **p < 0.01, ***p < 0.001 (Mann-Whitey test). Data are representative of two (A, C–J) or at least three (B and K) independent experiments. Error bars represent SEM. See also Figure S6.

adoptive transfer of retrovirus-transduced cells and LCMV infection (Ray et al., 2015). The exact reasons behind the divergent observations from ours are unclear, but efficiency of gene silencing might be critical and gene dosing effects might lead to different results. Additionally, silencing of mTOR exerts a strong inhibitory effect on Th1 cell differentiation in LCMV infection

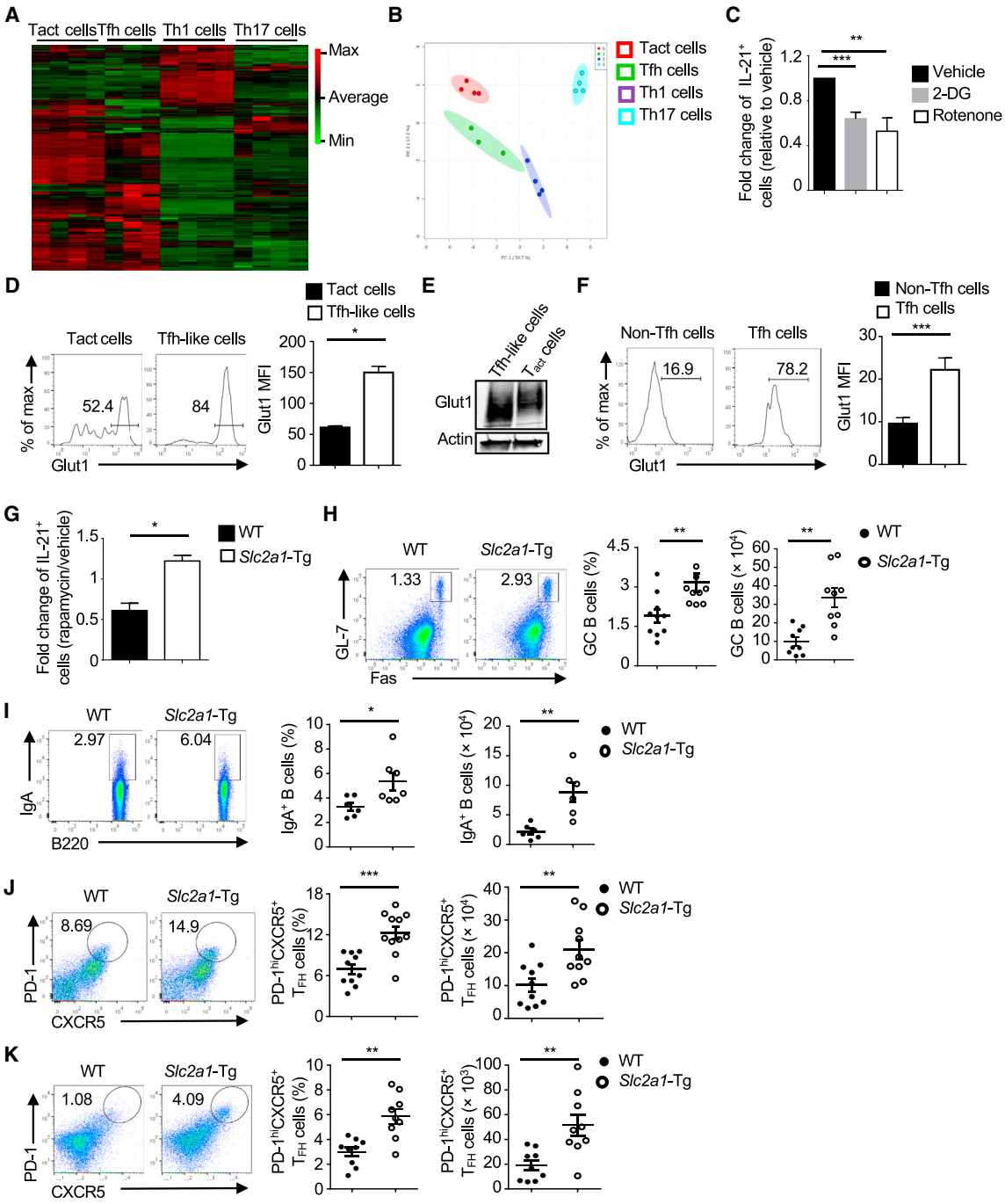

Figure 7. Glucose Metabolism Promotes Tfh Cell Differentiation

(A and B) Purified CD4$^+$ T cells were polarized in vitro to generate activated T cells (Tact), Tfh-like, Th1, and Th17 cells for high-resolution metabolomics analyses. The top 250 differentially observed metabolites are shown by heatmap (A) and principle component analysis (B).

(C) T cells were polarized in vitro to generate Tfh-like cells, in the presence of vehicle, 2-DG (250 μM), or rotenone (5 nM), for 3.5 days, followed by analysis of IL-21 expression. The fold change in the number of IL-21$^+$ CD4$^+$ cells in comparison to vehicle treated cells is shown.

(D and E) T cells were activated or polarized in vitro to generate Tfh-like cells for 3.5 days, followed by analysis of Glut1 expression by flow cytometry (D; right, the MFI of Glut1) or immunoblot (E).

(F) Flow cytometry of Glut1 expression on Tfh (B220$^-$CD4$^+$PD-1^{hi}CXCR5$^+$) and non-Tfh cells (B220$^-$CD4$^+$PD-1^{lo}CXCR5$^-$) from PPs. Right shows the MFI of Glut1.

(G) T cells from WT or *Slc2a1*-Tg mice were polarized in vitro to generate Tfh-like cells. After 3 days, the cells were treated with vehicle (DMSO) or rapamycin (50 nM) for 20 hr, followed by analysis of IL-21 expression. Graph represents the fold change in the number of IL-21$^+$ CD4$^+$ cells as a result of rapamycin treatment compared with that of vehicle treatment.

(legend continued on next page)

(Ray et al., 2015), suggesting that Tfh and Th1 cells could have different sensitivity to reduced mTOR activity. We also note that our results using PTEN-deficient or PI3K over-activation mice are consistent with previous studies that show a positive role of PI3K signaling in Tfh cell differentiation (Gigoux et al., 2009; Rolf et al., 2010).

Recent studies highlight distinct metabolic requirements for different T cell states and fates (MacIver et al., 2013). Our studies show that while Tfh cells utilize and require oxidative metabolism, glucose uptake and glycolysis are also important and can promote Tfh cell differentiation in vivo. Bcl6, the master regulator for Tfh cells, has been shown to inhibit glycolysis in vitro (Oestreich et al., 2014). Compared to Th1 cells, Tfh cells exhibit lower rates of glycolysis and oxidative phosphorylation (Ray et al., 2015). Conversely, Bcl6 expression and Tfh cells are associated with elevated cell proliferation (Kitano et al., 2011; Lüthje et al., 2012), demonstrating a use of anabolic metabolism. We show here that Tfh cell differentiation required the interplay between immune signaling from ICOS-mTOR or Tfh cell-promoting cytokines and metabolic reprogramming. This is reminiscent of the role of IL-2-mTORC1-mediated metabolism in orchestrating Treg cell proliferation and suppressive activity (Zeng et al., 2013). Our conclusion is further supported by results from inhibition of Myc or increased Glut1 expression, which directly illustrate the crucial role of anabolic metabolism in Tfh cell differentiation. Tfh cells might utilize this mixed metabolism to support both proliferation and cellular longevity while not depleting nutrients in GCs.

In summary, our study has identified the crucial roles of mTORC1 and mTORC2 in linking ICOS signals to metabolic and transcriptional regulation as a key mechanism for Tfh cell differentiation under various contexts. Tfh cells play an important role in humoral immunity but also contribute to autoimmune diseases. Our results suggest that clinical manipulation of Tfh cells could be accomplished by targeting mTOR signaling or metabolic pathways for therapeutic intervention of immune-mediated diseases.

EXPERIMENTAL PROCEDURES

Animals

All mice were kept in specific pathogen-free condition in Animal Resource Center at St. Jude Children's Research Hospital and Duke University. All animal protocols were approved by appropriate Institutional Animal Care and Use Committees. Further information is included in the Supplemental Experimental Procedures.

Tfh-like Cell Culture

Tfh-like cells were generated as described (Awe et al., 2015). Naive $CD4^+$ T cells were isolated by magnetic beads and cultured on anti-CD3 (10 μg/ml) and anti-CD28 (10 μg/ml)-coated plates in RPMI-1640 media supplemented with 10% FBS, sodium pyruvate, penicillin/streptomycin, HEPES, and β-mercaptoethanol for 3.5 days. The following cytokines were added to generate Tfh-like subset: 100 ng/ml IL-6 (eBioscience), 50 ng/ml IL-21 (R&D Systems), 10 μg/ml of each anti-IL-2, anti-IFN-γ (eBioscience), anti-IL-4 (eBioscience, clone 11B11), and anti-TGF-β (eBioscience) (Awe et al., 2015) (Awe et al., 2015). In some experiments, cells were treated with 5 nM rotenone, 250 μM 2-DG, rapamycin (50 nM), or DMSO vehicle.

Flow Cytometry

For analysis of surface markers, cells were stained in PBS containing 2% (wt/vol) fetal bovine serum (FBS). Flow cytometry data were acquired on LSRII or LSR Fortessa (BD Biosciences) or MACSQuant (Miltenyi) and analyzed using Flowjo software (Tree Star). Further information is included in the Supplemental Experimental Procedures.

Immunofluorescence

Fresh frozen PPs were cryosectioned, stained with antibodies, and imaged using Nikon TiE inverted microscope and an EMCCD camera (Andor). To analyze Foxo1 intracellular localization, we fixed, permeabilized, and stained cells with antibodies, imaged using a Marianis spinning disk confocal microscope (Intelligent Imaging Innovations) and EMCCD camera, and analyzed using Slidebook software (Intelligent Imaging Innovations). Details are included in the Supplemental Experimental Procedures.

Fecal IgA Measurement

Fecal pellets were collected, weighed, and resuspended in PBS with complete protease inhibitor (Roche) at 100 mg/ml. The tubes were taped horizontally on a vortex and shake vigorously for 10 min. The suspensions were centrifuged at 400 g for 5 min to pellet large debris. Supernatants were filtered through a 70 μM cell strainer, and the flow-through was collected and centrifuged at 8,000 g for 5 min. Supernatants were collected and IgA concentration was measured by ELISA (eBioscience).

ICOS Stimulation

After 3 days activation, live T cells were purified using Ficoll. Cells were rested for 3 hr and then incubated with anti-ICOS (5 μg/ml; C398.4A; Biolegend) followed by crosslinking with goat anti-hamster antibody (Jackson ImmunoResearch).

Metabolic Flux Analysis

Glycolytic flux was determined by measuring the detritiation of [3-^{3}H] glucose (Shi et al., 2011). De novo lipogenesis was measured as described before (Zeng et al., 2013). Details are included in the Supplemental Experimental Procedures.

Metabolomics

Metabolomic analyses were performed using LC Q Exactive Mass Spectrometer (LC-QE-MS) (Thermo Scientific) (Liu et al., 2014). MetaboAnalyst was used to analyze range-scale data and provide PCA and KEGG pathway analysis of metabolites significantly changed (1.5-fold difference, $p < 0.05$) (www.metaboanalyst.ca/).

Gene-Expression Profiling

Details are included in the Supplemental Experimental Procedures.

Statistical Analysis

p values were calculated with unpaired Student's t test, Mann-Whitney test, or analysis of variance (GraphPad Prism) as specified in figure legends, with proper post-test analysis performed.

ACCESSION NUMBERS

The microarray data are available in the Gene Expression Omnibus (GEO) database under the accession number GSE85555.

(H–J) Flow cytometry of GC B cells (H), IgA^+ B cells (I), and Tfh cells (J) in PPs from WT and *Slc2a1*-Tg mice. Right shows the frequency and number of indicated cell population.

(K) Flow cytometry of Tfh cells in the draining lymph nodes of WT and *Slc2a1*-Tg mice at day 10 after immunization with KLH. $^*p < 0.05$, $^{**}p < 0.01$ (Student's t test). Data are representative of three (C and D) or pooled from at least three (A, B, G–K) or five (E and F) independent experiments. Error bars represent SEM. See also Figure S7.

SUPPLEMENTAL INFORMATION

Supplemental Information includes seven figures, one table, and Supplemental Experimental Procedures and can be found with this article online at http://dx.doi.org/10.1016/j.immuni.2016.08.017.

AUTHOR CONTRIBUTIONS

H.Z. designed and performed experiments with Raptor, Rictor, PTEN, and Myc mutant mice and wrote the manuscript; S.C. designed and performed Glut1 mutant mouse and metabolic experiments and wrote the manuscript; C.G. performed imaging assays; G.N. performed bioinformatics analyses; S.S. performed LCMV infection; S.A.B. and C.C. performed immunoglobulin ELISA; R.J.K. assisted with immune experiments; X.G. and J.W.L. performed metabolomics analyses; B.Y., M.D., and M.O.L. provided reagents and insights; and J.C.R. and H.C. designed experiments, wrote the manuscript, and provided overall direction.

ACKNOWLEDGMENTS

The authors acknowledge N. Chapman and H. Shi for help with immunological assays, Y. Wang for editing the manuscript, and St. Jude Immunology FACS core facility for cell sorting. This work was supported by NIH AI105887, AI101407, CA176624, and NS064599, American Asthma Foundation, and Crohn's & Colitis Foundation of America (to H.C.), Alliance for Lupus Research and NIH DK105550 (to J.C.R.), and R01 CA193256 (to J.W.L).

Received: December 15, 2015
Revised: May 25, 2016
Accepted: June 13, 2016
Published: September 13, 2016

REFERENCES

Awe, O., Hufford, M.M., Wu, H., Pham, D., Chang, H.C., Jabeen, R., Dent, A.L., and Kaplan, M.H. (2015). PU.1 Expression in T Follicular Helper Cells Limits CD40L-Dependent Germinal Center B Cell Development. J. Immunol. *195*, 3705–3715.

Bollig, N., Brüstle, A., Kellner, K., Ackermann, W., Abass, E., Raifer, H., Camara, B., Brendel, C., Giel, G., Bothur, E., et al. (2012). Transcription factor IRF4 determines germinal center formation through follicular T-helper cell differentiation. Proc. Natl. Acad. Sci. USA *109*, 8664–8669.

Chi, H. (2012). Regulation and function of mTOR signalling in T cell fate decisions. Nat. Rev. Immunol. *12*, 325–338.

Choi, Y.S., Gullicksrud, J.A., Xing, S., Zeng, Z., Shan, Q., Li, F., Love, P.E., Peng, W., Xue, H.H., and Crotty, S. (2015). LEF-1 and TCF-1 orchestrate T(FH) differentiation by regulating differentiation circuits upstream of the transcriptional repressor Bcl6. Nat. Immunol. *16*, 980–990.

Chung, Y., Tanaka, S., Chu, F., Nurieva, R.I., Martinez, G.J., Rawal, S., Wang, Y.H., Lim, H., Reynolds, J.M., Zhou, X.H., et al. (2011). Follicular regulatory T cells expressing Foxp3 and Bcl-6 suppress germinal center reactions. Nat. Med. *17*, 983–988.

Crotty, S. (2014). T follicular helper cell differentiation, function, and roles in disease. Immunity *41*, 529–542.

Deane, J.A., Kharas, M.G., Oak, J.S., Stiles, L.N., Luo, J., Moore, T.I., Ji, H., Rommel, C., Cantley, L.C., Lane, T.E., and Fruman, D.A. (2007). T-cell function is partially maintained in the absence of class IA phosphoinositide 3-kinase signaling. Blood *109*, 2894–2902.

Donahue, A.C., and Fruman, D.A. (2007). Distinct signaling mechanisms activate the target of rapamycin in response to different B-cell stimuli. Eur. J. Immunol. *37*, 2923–2936.

Fagarasan, S., Kawamoto, S., Kanagawa, O., and Suzuki, K. (2010). Adaptive immune regulation in the gut: T cell-dependent and T cell-independent IgA synthesis. Annu. Rev. Immunol. *28*, 243–273.

Finlay, D., and Cantrell, D.A. (2011). Metabolism, migration and memory in cytotoxic T cells. Nat. Rev. Immunol. *11*, 109–117.

Finlay, D.K., Rosenzweig, E., Sinclair, L.V., Feijoo-Carnero, C., Hukelmann, J.L., Rolf, J., Panteleyev, A.A., Okkenhaug, K., and Cantrell, D.A. (2012). PDK1 regulation of mTOR and hypoxia-inducible factor 1 integrate metabolism and migration of CD8+ T cells. J. Exp. Med. *209*, 2441–2453.

Gigoux, M., Shang, J., Pak, Y., Xu, M., Choe, J., Mak, T.W., and Suh, W.K. (2009). Inducible costimulator promotes helper T-cell differentiation through phosphoinositide 3-kinase. Proc. Natl. Acad. Sci. USA *106*, 20371–20376.

Hedrick, S.M., Hess Michelini, R., Doedens, A.L., Goldrath, A.W., and Stone, E.L. (2012). FOXO transcription factors throughout T cell biology. Nat. Rev. Immunol. *12*, 649–661.

Iiyama, R., Kanai, T., Uraushihara, K., Totsuka, T., Nakamura, T., Miyata, T., Yagita, H., Kushi, A., Suzuki, K., Tezuka, K., and Watanabe, M. (2003). The role of inducible co-stimulator (ICOS)/B7-related protein-1 (B7RP-1) interaction in the functional development of Peyer's patches. Immunol. Lett. *88*, 63–70.

Jacobs, S.R., Herman, C.E., Maciver, N.J., Wofford, J.A., Wieman, H.L., Hammen, J.J., and Rathmell, J.C. (2008). Glucose uptake is limiting in T cell activation and requires CD28-mediated Akt-dependent and independent pathways. J. Immunol. *180*, 4476–4486.

Kang, S.G., Liu, W.H., Lu, P., Jin, H.Y., Lim, H.W., Shepherd, J., Fremgen, D., Verdin, E., Oldstone, M.B., Qi, H., et al. (2013). MicroRNAs of the miR-17∼92 family are critical regulators of T(FH) differentiation. Nat. Immunol. *14*, 849–857.

Kerdiles, Y.M., Beisner, D.R., Tinoco, R., Dejean, A.S., Castrillon, D.H., DePinho, R.A., and Hedrick, S.M. (2009). Foxo1 links homing and survival of naive T cells by regulating L-selectin, CCR7 and interleukin 7 receptor. Nat. Immunol. *10*, 176–184.

Kerdiles, Y.M., Stone, E.L., Beisner, D.R., McGargill, M.A., Ch'en, I.L., Stockmann, C., Katayama, C.D., and Hedrick, S.M. (2010). Foxo transcription factors control regulatory T cell development and function. Immunity *33*, 890–904.

Kitano, M., Moriyama, S., Ando, Y., Hikida, M., Mori, Y., Kurosaki, T., and Okada, T. (2011). Bcl6 protein expression shapes pre-germinal center B cell dynamics and follicular helper T cell heterogeneity. Immunity *34*, 961–972.

Klinger, M., Kim, J.K., Chmura, S.A., Barczak, A., Erle, D.J., and Killeen, N. (2009). Thymic OX40 expression discriminates cells undergoing strong responses to selection ligands. J. Immunol. *182*, 4581–4589.

Linterman, M.A., Pierson, W., Lee, S.K., Kallies, A., Kawamoto, S., Rayner, T.F., Srivastava, M., Divekar, D.P., Beaton, L., Hogan, J.J., et al. (2011). Foxp3+ follicular regulatory T cells control the germinal center response. Nat. Med. *17*, 975–982.

Liu, X., Ser, Z., and Locasale, J.W. (2014). Development and quantitative evaluation of a high-resolution metabolomics technology. Anal. Chem. *86*, 2175–2184.

Lüthje, K., Kallies, A., Shimohakamada, Y., Belz, G.T., Light, A., Tarlinton, D.M., and Nutt, S.L. (2012). The development and fate of follicular helper T cells defined by an IL-21 reporter mouse. Nat. Immunol. *13*, 491–498.

Macintyre, A.N., Gerriets, V.A., Nichols, A.G., Michalek, R.D., Rudolph, M.C., Deoliveira, D., Anderson, S.M., Abel, E.D., Chen, B.J., Hale, L.P., and Rathmell, J.C. (2014). The glucose transporter Glut1 is selectively essential for CD4 T cell activation and effector function. Cell Metab. *20*, 61–72.

MacIver, N.J., Michalek, R.D., and Rathmell, J.C. (2013). Metabolic regulation of T lymphocytes. Annu. Rev. Immunol. *31*, 259–283.

Nakayamada, S., Kanno, Y., Takahashi, H., Jankovic, D., Lu, K.T., Johnson, T.A., Sun, H.W., Vahedi, G., Hakim, O., Handon, R., et al. (2011). Early Th1 cell differentiation is marked by a Tfh cell-like transition. Immunity *35*, 919–931.

Oestreich, K.J., Read, K.A., Gilbertson, S.E., Hough, K.P., McDonald, P.W., Krishnamoorthy, V., and Weinmann, A.S. (2014). Bcl-6 directly represses the gene program of the glycolysis pathway. Nat. Immunol. *15*, 957–964.

Ouyang, W., Beckett, O., Flavell, R.A., and Li, M.O. (2009). An essential role of the Forkhead-box transcription factor Foxo1 in control of T cell homeostasis and tolerance. Immunity *30*, 358–371.

Ouyang, W., Beckett, O., Ma, Q., Paik, J.H., DePinho, R.A., and Li, M.O. (2010). Foxo proteins cooperatively control the differentiation of Foxp3+ regulatory T cells. Nat. Immunol. *11*, 618–627.

Ouyang, W., Liao, W., Luo, C.T., Yin, N., Huse, M., Kim, M.V., Peng, M., Chan, P., Ma, Q., Mo, Y., et al. (2012). Novel Foxo1-dependent transcriptional programs control T(reg) cell function. Nature *491*, 554–559.

Pollizzi, K.N., Patel, C.H., Sun, I.H., Oh, M.H., Waickman, A.T., Wen, J., Delgoffe, G.M., and Powell, J.D. (2015). mTORC1 and mTORC2 selectively regulate $CD8^+$ T cell differentiation. J. Clin. Invest. *125*, 2090–2108.

Ray, J.P., Staron, M.M., Shyer, J.A., Ho, P.C., Marshall, H.D., Gray, S.M., Laidlaw, B.J., Araki, K., Ahmed, R., Kaech, S.M., and Craft, J. (2015). The Interleukin-2-mTORc1 Kinase Axis Defines the Signaling, Differentiation, and Metabolism of T Helper 1 and Follicular B Helper T Cells. Immunity *43*, 690–702.

Rolf, J., Bell, S.E., Kovesdi, D., Janas, M.L., Soond, D.R., Webb, L.M., Santinelli, S., Saunders, T., Hebeis, B., Killeen, N., et al. (2010). Phosphoinositide 3-kinase activity in T cells regulates the magnitude of the germinal center reaction. J. Immunol. *185*, 4042–4052.

Shen, W.H., Balajee, A.S., Wang, J., Wu, H., Eng, C., Pandolfi, P.P., and Yin, Y. (2007). Essential role for nuclear PTEN in maintaining chromosomal integrity. Cell *128*, 157–170.

Shi, L.Z., Wang, R., Huang, G., Vogel, P., Neale, G., Green, D.R., and Chi, H. (2011). HIF1alpha-dependent glycolytic pathway orchestrates a metabolic checkpoint for the differentiation of TH17 and Treg cells. J. Exp. Med. *208*, 1367–1376.

Shrestha, S., Yang, K., Guy, C., Vogel, P., Neale, G., and Chi, H. (2015). Treg cells require the phosphatase PTEN to restrain TH1 and TFH cell responses. Nat. Immunol. *16*, 178–187.

Song, M.S., Carracedo, A., Salmena, L., Song, S.J., Egia, A., Malumbres, M., and Pandolfi, P.P. (2011). Nuclear PTEN regulates the APC-CDH1 tumor-suppressive complex in a phosphatase-independent manner. Cell *144*, 187–199.

Srinivasan, L., Sasaki, Y., Calado, D.P., Zhang, B., Paik, J.H., DePinho, R.A., Kutok, J.L., Kearney, J.F., Otipoby, K.L., and Rajewsky, K. (2009). PI3 kinase signals BCR-dependent mature B cell survival. Cell *139*, 573–586.

Stone, E.L., Pepper, M., Katayama, C.D., Kerdiles, Y.M., Lai, C.-Y.Y., Emslie, E., Lin, Y.C., Yang, E., Goldrath, A.W., Li, M.O., et al. (2015). ICOS coreceptor signaling inactivates the transcription factor FOXO1 to promote Tfh cell differentiation. Immunity *42*, 239–251.

Wang, R., Dillon, C.P., Shi, L.Z., Milasta, S., Carter, R., Finkelstein, D., McCormick, L.L., Fitzgerald, P., Chi, H., Munger, J., and Green, D.R. (2011). The transcription factor Myc controls metabolic reprogramming upon T lymphocyte activation. Immunity *35*, 871–882.

Weber, J.P., Fuhrmann, F., Feist, R.K., Lahmann, A., Al Baz, M.S., Gentz, L.J., Vu Van, D., Mages, H.W., Haftmann, C., Riedel, R., et al. (2015). ICOS maintains the T follicular helper cell phenotype by down-regulating Krüppel-like factor 2. J. Exp. Med. *212*, 217–233.

Xiao, N., Eto, D., Elly, C., Peng, G., Crotty, S., and Liu, Y.-C.C. (2014). The E3 ubiquitin ligase Itch is required for the differentiation of follicular helper T cells. Nat. Immunol. *15*, 657–666.

Yang, K., Shrestha, S., Zeng, H., Karmaus, P.W., Neale, G., Vogel, P., Guertin, D.A., Lamb, R.F., and Chi, H. (2013). T cell exit from quiescence and differentiation into Th2 cells depend on Raptor-mTORC1-mediated metabolic reprogramming. Immunity *39*, 1043–1056.

Yusuf, I., Kageyama, R., Monticelli, L., Johnston, R.J., Ditoro, D., Hansen, K., Barnett, B., and Crotty, S. (2010). Germinal center T follicular helper cell IL-4 production is dependent on signaling lymphocytic activation molecule receptor (CD150). J. Immunol. *185*, 190–202.

Zeng, H., Yang, K., Cloer, C., Neale, G., Vogel, P., and Chi, H. (2013). mTORC1 couples immune signals and metabolic programming to establish T(reg)-cell function. Nature *499*, 485–490.